

Aberration analysis and efficiency improvement of a bidirectional optical subassembly

Hao Wu
Zhangdi Huang
Ziyan Yu
Xiaoshi Qian
Fei Xu
Nanjing University
Department of Material Science and Engineering
and National Laboratory of Solid State
Microstructures
22 Hankou Road
Nanjing, 210093
China

Beckham Chen
Light Master Technology (Ningbo) Inc.
eGtran Group
No. 3 Yangzi River Road South Area
Ningbo Free Trade Zone
China

Yanqing Lu
Nanjing University
Department of Material Science and Engineering
and National Laboratory of Solid State
Microstructures
22 Hankou Road
Nanjing, 210093
China
and
Light Master Technology (Ningbo) Inc.
eGtran Group
No. 3 Yangzi River Road South Area
Ningbo Free Trade Zone
China
E-mail: yqlu@nju.edu.cn

Abstract. An approach to improve the coupling efficiency of bidirectional optical subassembly (BOSA) modules is proposed and experimentally demonstrated. We analyzed the wavefront aberration coefficients of a typical BOSA. It was found that the 45-deg wavelength filter induces coma and astigmatism, and then it further deteriorates the laser diode to fiber coupling. We measured the BOSA efficiencies based on a series of different filters. For a typical 0.5-mm filter, 25% coupling efficiency improvement was achieved by optimizing the filter parameters. © 2009 Society of Photo-Optical Instrumentation Engineers. [DOI: 10.1117/1.3251278]

Subject terms: bidirectional optical sub-assembly; fiber-to-the-home; aberration.

Paper 090460RR received Jun. 23, 2009; revised manuscript received Sep. 2, 2009; accepted for publication Sep. 4, 2009; published online Oct. 23, 2009.

1 Introduction

The explosive expansion of the Internet has accelerated the growth of optical communication. Right after the long-haul and metro networks, low-cost high-speed access optical network has been developing rapidly in recent years.¹⁻⁹ Optical fibers are replacing copper wires to overcome the "first-mile bottleneck." The final goal of fiber-to-the-home is to provide an optical fiber from the central office to each customer's premises or home, which is typically a distance of <20 km.^{1,2}

In the electrical domain, at least two wires (coax, twisted pair, etc.) are needed in order to establish a link. For a complete bidirectional copper link, we either need more wires or multiplexing technologies that separate the traffic into different directions. In the optical world, the situation is somewhat different. A single fiber can fulfill the demand

of bidirectional transmitting because photons do not superimpose (collide) when being sent at different wavelengths in the same fiber.

Single-fiber designs save overall system costs because only one fiber is needed. This is quite attractive for a cost-sensitive access network. To date, single-fiber bidirectional optical transceivers have dominated the market,¹ while the bidirectional optical subassembly (BOSA) is the core function unit inside it. However, one disadvantage emerges when BOSA is employed in comparison to a transmitting optical subassembly (TOSA). The laser diode (LD) to the fiber coupling efficiency of a BOSA is much lower than that of a TOSA, even with the same LD and fiber. Higher-power LDs thus have to be used. As a consequence, it is quite important to figure out the origin to worse coupling and the way to improve the efficiency. To the best of our knowledge, no such detailed analysis has been reported in technical literature.

In this paper, the characteristic of geometrical ray aberration inside a typical BOSA was studied theoretically. We

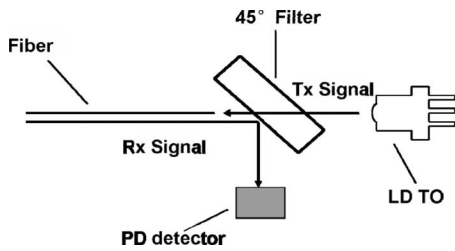


Fig. 1 Schematic of a typical BOSA.

found the coma and astigmatism caused by the plane-parallel wavelength filter affect the mode-coupling from a LD to a fiber. By adjusting the filter's thickness and refractive index, ~25% transmission efficiency enhancement has been experimentally demonstrated.

2 Ray Aberration Analysis of a BOSA

In a typical transceiver, BOSA is the most critical function unit, which covers ~70% of total transceiver cost. Figure 1 shows a two-port BOSA configuration containing three key parts: a LD with a transistor outline (TO) package (LDTO), a receiving photodiode (PD) detector, and a common optical fiber. Normally, the LDTO has a lens cap. The lens could be in a ball shape or with a specially designed aspherical surface for better coupling. With the help of lens cap, emitting light from a LD is converged and then travels through a wavelength selective filter into an optical fiber (Tx signal). On the receiver side, light with a different wavelength comes from the same fiber into the module, is reflected by the filter and received at a detector (Rx signal). At the other end of the fiber, a complementary module is used in order to complete the optical link. A single-wavelength bidirectional system is also possible. However, a beamsplitter instead of a wavelength filter should be used in such a BOSA. An advantage is that identical modules can be used at both sides with a resulting cost reduction. However, a higher cross-talk would be induced.

In a BOSA, a wavelength filter or a beamsplitter is normally a glass plate with a specified coating. The filter/beamsplitter plays an important role to realize BOSA functions. Either the orientation or spectral properties may prominently affect a BOSA's performance. High-quality coating and precise positioning are required. However, it is found that a BOSA's LD-to-fiber coupling efficiency is always lower than that of a simple TOSA if the same LD and fiber are used. Because the wavelength filter is the only extra component between the LDTO and the fiber, one would speculate that the beam might be skewed due to the filter, and then the light coupling to fiber is affected.

Because the Rx part of a BOSA is normally at the side of module housing, the optical filter should be placed at a ~45-deg angle to reflect beam toward the PD detector. The filter thickness is normally about 0.3–0.6 mm made with BK7 or similar glasses. A filter thinner than 0.3 mm is relatively difficult to fabricate.

To analyze the aberration induced by an oblique filter, we treat it like a tilted plane-parallel plate and neglect the coating's effects. Actually, the coating only affects the propagation loss, which could easily reach >95%.

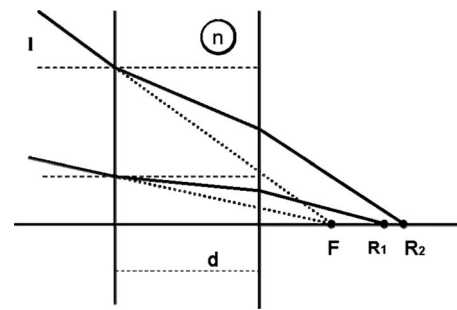


Fig. 2 Ray aberration induced by a tilted plane parallel plate.

Figure 2 shows an incident converging pencil of rays traveling in air and focused in point F. A plane parallel plate with refractive index n is inserted in the pencil so that the outgoing beam suffers aberration. Assuming the original converged wavefront is a pure sphere, all beams could be focused. However, after the filter is employed, beams with different incident angles may not shoot to a unique focus, which are shown in Fig. 2 with point R_1 , R_2 , etc. Different focusing points mean aberration. The wavefront in the exit pupil thus is not a perfect sphere; therefore, different parts of the wavefront come to focus in different points, as shown in Fig. 3.

We can define wavefront aberration W as the optical path difference between the aberrated and the ideal unaberrated wavefronts. If we express the wavefront aberration with the Zernike polynomials in a polar system, it can be written as follows:¹⁰

$$\begin{aligned}
 W(\rho, \theta') = & Z_0 + Z_1\rho \cos \theta' + Z_2\rho \sin \theta' + Z_3(2\rho^2 - 1) \\
 & + Z_4\rho^2 \cos 2\theta' + Z_5\rho^2 \sin 2\theta' \\
 & + Z_6(3\rho^2 - 2)\rho \cos \theta' + Z_7(3\rho^2 - 2)\rho \sin \theta' \\
 & + Z_8(6\rho^4 - 6\rho^2 + 1).
 \end{aligned}
 \tag{1}$$

In this expression, ρ and θ' are orthogonal in a continuous fashion over the interior of a unit circle. Z_0 – Z_8 are the first nine Zernike terms.

To compute the aberration of a tilted plane parallel plate, a number of parameters should be taken into account, including the plate refractive index n , thickness d , the filter tilting angle α , and beams' maximum converging angle

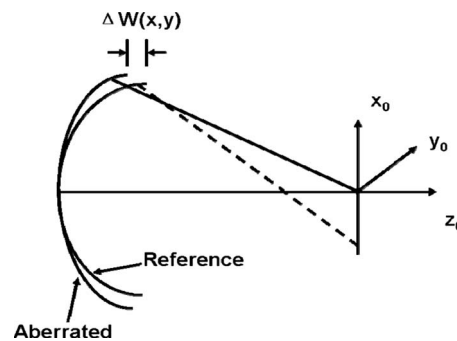


Fig. 3 Spherical reference wavefront having a focus at the origin of the coordinate system (x_0, y_0, z_0) and an aberrated wavefront that may not have a unique focus.

[i.e., numerical aperture (NA) if it is not too large.¹⁰⁻¹²] Final expressions for the aberration terms of a tilted plane-parallel plate by means of W_{lm} can be given in following forms.¹¹

The lowest-order spherical-aberration:

$$W_{40} = \frac{1}{8(n^2 - \sin^2 \alpha)^{7/2}} \left[\cos^2 \alpha (n^2 - \sin^2 \alpha) - \frac{1}{8} (3 \sin^4 \alpha + 8 \cos^4 \alpha - 6 \sin^2 2\alpha) \times (n^2 - \sin^2 \alpha)^2 - \frac{3}{16} (4 \cos^2 \alpha - 3 \sin^2 \alpha) \times \sin^2 2\alpha (n^2 - \sin^2 \alpha) - \frac{15}{128} \sin^4 2\alpha \right] d(\text{NA})^4 \quad (2)$$

The third-order coma:

$$W_{31} = - \frac{(n^2 - 1)[n^2 - (\sin^2 \alpha)/4] \sin 2\alpha}{4(n^2 - \sin^2 \alpha)^{5/2}} d(\text{NA})^3 \quad (3)$$

The lowest-order astigmatic term:

$$W_{22} = \frac{(n^2 - 1) \sin^2 \alpha}{4(n^2 - \sin^2 \alpha)^{3/2}} d(\text{NA})^2 \quad (4)$$

For cubic coma, we find

$$W_{33} = - \frac{(n^2 - 1) \sin^2 \alpha \sin 2\alpha}{16(n^2 - \sin^2 \alpha)^{5/2}} d(\text{NA})^3 \quad (5)$$

The expression for fifth-order astigmatism is

$$W_{42} = - \frac{\sin^2 \alpha}{16(n^2 - \sin^2 \alpha)^{7/2}} [(\sin^2 \alpha - 6 \cos^2 \alpha) \times (n^2 - \sin^2 \alpha)^2 + 6 \cos 2\alpha \cos^2 \alpha (n^2 - \sin^2 \alpha) + 5 \cos^4 \alpha \sin^2 \alpha] d(\text{NA})^5. \quad (6)$$

The fifth-order linear coma can be written as

$$W_{51} = \frac{\sin 2\alpha}{16(n^2 - \sin^2 \alpha)^{9/2}} \left[\frac{35}{128} \sin^4 2\alpha - \frac{5}{16} \times (5 \sin^2 \alpha - 6 \cos^2 \alpha)(n^2 - \sin^2 \alpha) \sin^2 \alpha + \frac{3}{8} \times (8 \cos^4 \alpha - 24 \sin^2 \alpha \cos^2 \alpha + 5 \sin^4 \alpha) \times (n^2 - \sin^2 \alpha)^2 - \frac{1}{2} (4 \cos^2 \alpha - 3 \sin^2 \alpha) \times (n^2 - \sin^2 \alpha)^3 - (n^2 - \sin^2 \alpha)^4 \right] d(\text{NA})^5. \quad (7)$$

These coefficients actually tell us the wavefront aberration of every given ray in the exit pupil plane.¹¹ It is clear from (2)–(7) that severe aberration is induced with the increase of filter thickness and ray converging angle. Figure 4 shows the dependence of the aberration coefficients on n , where we assume the filter tilting angle α is 45 deg, the

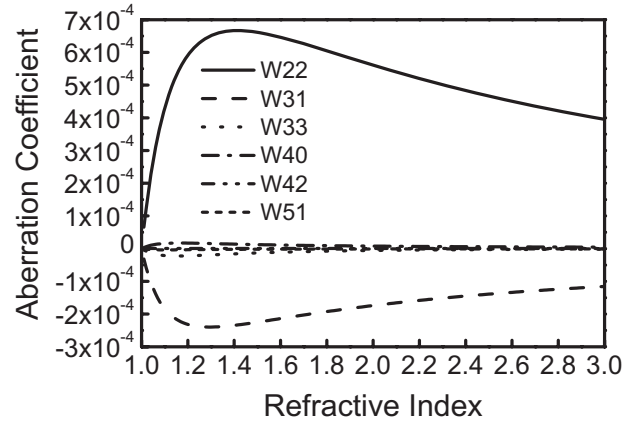


Fig. 4 Wavefront aberration coefficients as a function of filter index n .

thickness $d=0.5$ mm, and the numerical aperture NA = 0.14, which is the typical value of a single mode fiber for BOSA application.

It can be seen from the curve that the third-order linear coma and the lowest-order astigmatism are the most serious aberrations, which are greatly larger than the other three kinds of aberrations. Because the optical fiber has rotational symmetry, the unsymmetrical aberration—coma W_{31} and astigmatism W_{22} —should have the worst impact on the light coupling to a fiber.

It is interesting to see from Fig. 4 that the contribution of n does not show a simple curve. As n increases from 1 to 1.4, the amount of lowest-order astigmatism W_{22} increases, while as n increases beyond 1.4, the amount of W_{22} decreases gradually. A similar trend can be found in other aberration coefficients. The only differences are the peak positions. The third-order linear coma W_{31} reaches its maxima when n equals 1.28, while W_{40} , W_{51} , and W_{33} have peaks at $n=1.2$, 1.18, and 1.18, respectively.

It is obvious that the aberrations are negligible if the filter's index is 1, which means no filter is employed; therefore, the aberration disappears. However, it is interesting to see the low aberration at high indices. With the help of a simple illustration, one could figure out that the rays inside the plate travel nearly along the normal to the surface if the refractive index goes very large. In this case, all rays are displaced approximately the same amount. An exact mapping of the wavefront (or rays) between the two surfaces is thus obtained. That is a explanation of low aberration at a high n , whereas Fig. 4 tell us the aberration peak positions, which corresponds to the worst focusing.

In a real BOSA, the filter thickness, tilting angle, and beam's converging angle might be different, but the basic trend of aberration versus n should be the same. As we know, glasses such as BK7 and D263 are normally selected as filter substrate. Their indices at telecom bands are normally between 1.4 and 1.5, which are very close to the peak positions in Fig. 4. Thus, from our analysis, even if the LDTO's lens cap is an ideal lens, the filter still generates strong aberration, thus a low LD-to-fiber coupling will be predicted. To improve the coupling efficiency, either a thin substrate could be used or we may select more suitable materials. Because glasses with refractive index of <1.3

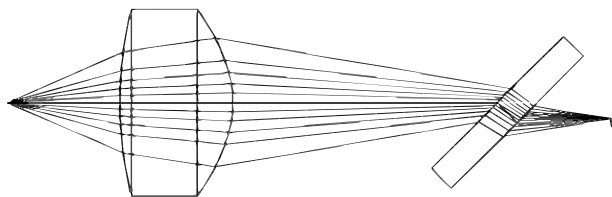


Fig. 5 Zemax modeling of the transmitting part in a typical BOSA.

are not popular, we may use high-index materials instead. Among them, silicon might be a choice. Its index at $1.55 \mu\text{m}$ is ~ 3.5 , which is quite larger than BK7. From Fig. 4, half the amount of W_{22} is expected. A higher LD-to-fiber coupling is thus achievable.

3 Zemax™ Simulation of a BOSA's Coupling Efficiency

To further investigate the filter-induced aberration and fiber coupling, Zemax simulation of a typical BOSA is done as shown in Fig. 5. Zemax is a widely used commercial software that can model, analyze, and optimize the design of various optical systems. Other similar programs such as Code_V, ASAP also could be used to model fiber optic components.

As shown in Fig. 5, a dispersed beam is generated by a LD then focused by an aspherical lens cap. The object space NA is set at 0.4 to simulate a typical LD. The lens's back focal length is 3.5 mm. A 0.3-mm, 45-deg tilted plane-parallel plate of refractive index n is inserted in the pencil of rays as a wavelength filter. It is obvious that the beam is deflected by the filter so that the optical fiber (not shown in Fig. 5.) should make a lateral offset for light coupling.

Figure 6(a) is the spot diagram of a BK7 filter-based BOSA while Fig. 6(b) is that of a silicon filter. The spot diagram shows the ray's distribution of one ideal spot object on the image plane. Obviously, these two systems both have some unsymmetrical aberration, such as coma and astigmatism, caused by the filters.

For a BK7 filter-based BOSA, the root-mean-square (rms) spot radius is $5.5 \mu\text{m}$, which is much larger than that of a silicon filter, which is reading $3.6 \mu\text{m}$ from the spot diagram. This means the image quality of a silicon filter system is much better than the former. More efficient coupling could be expected. Figure 7 shows the rms spot sizes

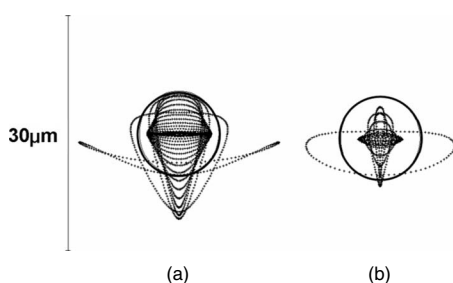


Fig. 6 Beam spot diagrams of two BOSAs with different filters. (a) BK7 (rms radius= $5.5 \mu\text{m}$), (b) Silicon (rms radius= $3.6 \mu\text{m}$). Evident coma and astigmatism aberrations could be identified in the diagrams. The circles in the spot diagrams represent Airy disks.

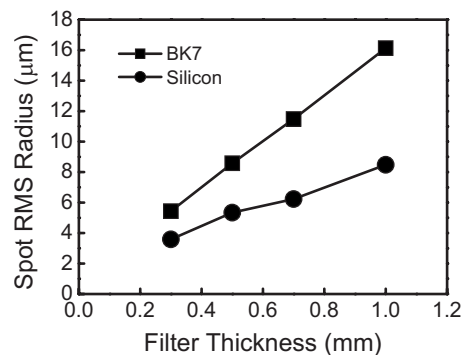


Fig. 7 The rms spot sizes of BOSAs with different filter materials and thicknesses (simulated with Zemax).

as a function of filter thicknesses for BK7 and silicon filter substrates, respectively. It exhibits a nearly linear trend, but BK7 always gives larger beam spots with different filter thicknesses.

However, to calculate the LD-to-fiber coupling efficiency precisely, the geometrical ray tracing is not adequate. The physical optics propagation (POP) algorithm should be used to compute fiber coupling efficiency. The beam's phase deviation is considered as the beams are transformed from one optical surface to another. In Zemax, the POP function has been included for years and used for numerous applications.

In a POP algorithm, the fiber coupling receiver efficiency is defined as a normalized overlap integral between the fiber mode distribution and the beam complex amplitude, which may be computed at the location of the receiving fiber,¹³⁻¹⁵

$$T = \frac{\left| \iint F_r(x,y) W^*(x,y) dx dy \right|^2}{\iint F_r(x,y) F_r^*(x,y) dx dy \iint W(x,y) W^*(x,y) dx dy}, \quad (8)$$

where $F_r(x,y)$ is the function describing the receiving fiber complex amplitude, $W(x,y)$ is the function describing the complex amplitude of the beam coupling into the fiber, and prime represents complex conjugate. Note that these functions are all complex valued; thus, this is a coherent overlap integral. Maximum receiver efficiency ($T=1.0$) is obtained when the mode of the beam perfectly matches the mode of the fiber in both amplitude and phase at all points. Any deviation in mode shape, or phase, will reduce the value of T to <1.0 . Optical aberrations typically introduce phase deviations, which reduce receiver efficiency. In a BOSA, the LDTO's lens cap is the most critical element that determines the LD-to-fiber coupling efficiency. Assume an LD chip has a beam waist of $2-3 \mu\text{m}$ at its emitting facet, a well-placed lens cap with ~ 4 times magnification factor are normally used for fiber coupling. In this case, the beam field may match fiber's mode field diameter, which is around $10 \mu\text{m}$ for ITU G.652 single-mode fibers.^{13,14} To date, people are using an aspherical lens for BOSA applications, especially in the optical line termination (OLT).

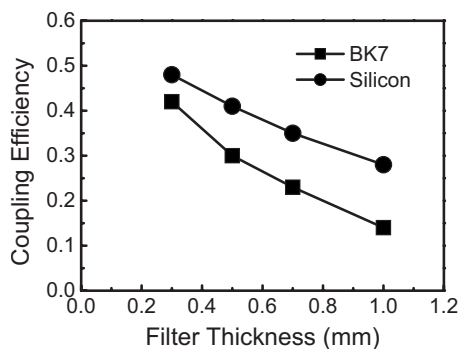


Fig. 8 BOSA coupling efficiencies (CEs) with different filter materials and filter thicknesses (simulated by Zemax).

However, commercially available LDTOs are just optimized for direct fiber coupling. The effects of the wavelength filter have not been counted intentionally. As a consequence, the wavefront aberration induces the mismatch between fiber mode and light field even if an ideal lens cap is used. The fiber coupling efficiency drops according to (8).

With the help of Zemax software, we studied the LD-to-fiber coupling of a BOSA shown in Fig. 8. A 0.3 mm BK7 filter based BOSA gives a coupling efficiency of 42% while a 48% efficiency could be obtained if the filter is made with silicon. A 14% efficiency enhancement could be expected, which is quite attractive. The higher index filter is very helpful based on both the ray-tracing and POP analysis.

To further study the effects of wavelength filter, the LD to fiber coupling efficiencies were also calculated at 0.5, 0.7, and 1 mm thicknesses, as shown in Fig. 8. The efficiency drops with thicker filters, but the silicon filters always have better results. For a 1-mm filter, if we choose silicon rather than BK7, the coupling efficiency is almost doubled. These results coincide well with the geometrical rms spot-size discussions in Fig. 7. A minor difference is that the efficiency does not show a linear relation any more with respect to filter thickness. One possible explanation is that the rms spot size can not always represent the real beam spot dimension. If the rms spot is smaller than the diffraction limit, an Airy disk size is closer to the real beam dimension. Therefore, the efficiency difference for BK7 and silicon filters becomes smaller for a thinner filter. In a word, the geometrical optics-based rms spot is suitable for quick analysis while POP gives the coupling efficiency values.

4 Experimental Results

Theoretical analysis reveals that the LD-to-fiber coupling efficiency could be adjusted by changing the wavelength filter's index and thickness, which gives us a straightforward way to improve a BOSA's performances. In this section, some experimental data are reported to testify the results.

A Mitsubishi ML920L16S DFB laser diode is selected for the experiments. It has an aspheric lens cap which is designed for LD-to-fiber coupling. Its emitting wavelength is at 1490 nm, which fulfills the OLT BOSA application. A Motech precise current source is used to drive the LD, which is plugged into a socket and then attached on a

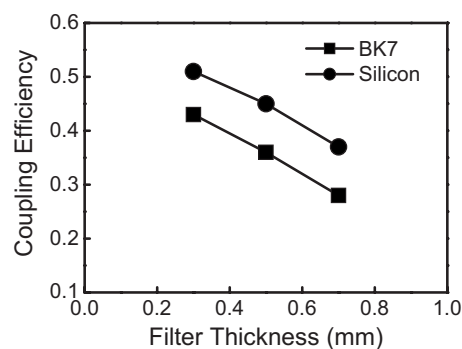


Fig. 9 BOSA CE's with different filter materials and filter thicknesses (experimental results).

Melles Griot 6-axis submicron moving and rotation stage. A single-mode optical fiber is placed at the focal points of the LDTO. A 45-deg tilted BK7 or silicon plate locates between the LD and fiber. Fine tuning is required to couple the LD's emitting light into the fiber. First of all, the LDTO itself was characterized by using an Agilent 8165B large-area power meter. The threshold current and slope efficiency are measured to be 8 mA and 0.25 mw/mA, respectively. Spectrum measurement shows that the LDTO has a center emitting wavelength at 1490 nm with a side-mode suppression ratio over 35 dB.

To measure the LD-to-fiber coupling efficiency, the LD slope efficiency after passing through a filter is measured as reference. Then, the light is coupling into a single-mode fiber by carefully adjusting the tuning stages. After the best coupling is reached, the slope efficiency is computed by measuring the light power that comes out from the other end of the fiber. The coupling efficiency is defined as the slope efficiency ratio with and without a wavelength filter.

A 0.3-mm BK7 filter was selected for the first efficiency measurement, which is 45%. Then it was replaced by a silicon filter with the same thickness. Measuring the coupling efficiency again, we found the efficiency increased to 51%, which represents a 13% improvement. The relative efficiency enhancement agrees well with the theoretical results described in Fig. 8. The small difference might be due to the deviation of the parts' parameters from their listed values. More experimental results could be found in Fig. 9 by using 0.5 and 0.7 mm filters. A similar trend was obtained that coincides with previous theoretical predictions. For 0.5 mm filters, the measured efficiencies are 36 and 45% for BK7 and silicon filters, respectively; for the thicker 0.7-mm filters, the efficiencies drop a lot due to the higher aberration caused by thicker plates. Only 28% (BK7) and 37% (silicon) efficiencies were achieved. However, silicon-based filters always perform better than BK7 filters. This quite matches the simulation results. Because the thin-film coating technology has been developed very well, coating on high-index substrates no longer has technical problems. We believe the high-index filter approach is really a good solution that may evidently improve the BOSA coupling efficiency while it does not affect the manufacturing processes.

5 Summary

An approach to increase the coupling efficiency of BOSA was proposed. According to the wavefront aberration coefficients of a tilted plane-parallel plate, the image quality is highly dependent on the refractive index n of the filter. As n increases beyond 1.4, every term of aberration decreases; thus, the image quality is improved resulting in a better coupling to the fiber.

To numerically compute the BOSA efficiency, Zemax simulations were fulfilled and then the results were verified with experiments. With the increase of filter thickness from 0.3 to 1.0 mm, the LD-to-fiber coupling efficiency drops severely but a high-index filter always shows much better results. When the filter thickness is 0.3 mm, using a silicon filter can improve the efficiency by 13%; whereas when $d=0.5$ and $d=0.7$ mm experimentally, 25 and 32% efficiency enhancement were achieved. Our theoretical and experimental results would be helpful for the design and development of high-performance fiber optic active components.

Acknowledgments

This work was sponsored by NSFC program under Contract No. 10874080, the Nature Science Foundation of Jiangsu Province under Contract No. BK2007712 and 973 program under Contracts No. 2006CB921805 and No. 2010CB327803. Lu acknowledges support from China MOE for the new century and Changjiang scholars program.

References

1. P. W. Shumate, "Fiber-to-the-home: 1977–2007," *J. Lightwave Technol.* **26**(9), 1093–1103 (2008).
2. F. Effenberger, D. Cleary, O. Haran, G. Kramer, R. D. Li, M. Oron,

- and T. Pfeiffer, "An introduction to PON technologies," *IEEE Commun. Mag.* **3**, 517–525 (2007).
3. C. H. Lee, "Fiber to the home using a PON infrastructure," *J. Lightwave Technol.* **24**(12), 4568–4583 (2006).
4. S. J. Park, C. H. Lee, K. T. Jeong, H. J. Park, J. G. Ahn, and K. H. Song, "Fiber-to-the-home services based on wavelength division multiplexing passive optical network," *J. Lightwave Technol.* **22**(11), 2582–2592 (2004).
5. J. Yoshida, "Low-cost optical modules for fiber-to-the-home," in *Lasers and Electro-Optics Soc. Annual Meeting*, IEEE, pp. 275–276 (1996).
6. T. T. Shih, M. C. Lin, P. H. Tseng, C. Y. Li, T. Y. Hung, and Y. J. Chiu, "High-performance and low-cost 10-Gb/s bidirectional optical subassembly modules," *J. Lightwave Technol.* **25**(11), 3488–3494 (2007).
7. A. Ohki, S. Fukushima, M. Sugo, K. Kato, and Y. Akatsu, "Development of TO-BOSA for FTTH using new optical path alignment technique," *Electron. Lett.* **43**(6), 57–58 (2007).
8. D. Shimura, R. Sekikawa, K. Kotani, M. Uekawa, Y. Maeno, K. Aoyama, H. Sasaki, T. Takamori, K. Masuko, and S. Nakaya, "Bidirectional optical subassembly with prealigned silicon microlens and laser diode," *IEEE Photonics Technol. Lett.* **18**(16), 1738–1840 (2006).
9. K. Masuko, T. Ori, T. Tanaka, and M. Inoue, "A low cost PON transceiver using single TO-CAN type micro-BOSA," in *Electronics Components and Technology Conf.*, IEEE, pp. 1082–1086, 2006.
10. J. C. Wyant and K. Creath, "Basic wave-front aberration theory for optical metrology," in *Applied Optics and Optical Engineering*, pp. 28–36, Academic Press, New York (1992).
11. J. Braat, "Analytical expressions for the wave-front aberration coefficients of a tilted plane-parallel plate," *Appl. Opt.* **36**(32), 8459–8467 (1997).
12. J. Eerenbeemd and S. Stallinga, "Compact system description for systems comprising a tilted plane parallel plate," *Appl. Opt.* **46**(3), 8459–8467 (2007).
13. H. Ghafoori-Shiraz and T. Asano, "Micro-lens for coupling a semiconductor laser to a single-mode fiber," *Opt. Lett.* **11**(8), 537–539 (1986).
14. M. Saruwatari and K. Nawata, "Semiconductor laser to single-mode fiber coupler," *Appl. Opt.* **18**(11), 1847–1856 (1979).
15. C. A. Edwards, H. M. Presby, and C. Dragone, "Ideal microlenses for laser to fiber coupling," *J. Lightwave Technol.* **11**(2), 252–257 (1993).

Biographies and photographs of authors not available.